Desalination and Water Treatment
www.deswater.com

doi: 10.5004/dwt.2020.24960

178 (2020) 312–321
February

Adsorption of Reactive Red 195 dye from industrial wastewater by dried soybean leaves modified with acetic acid

Hani Mahanna*, Mahmoud Samy

[a]*Public Works Engineering Department, Faculty of Engineering, Mansoura University, Mansoura, 35516, Egypt, emails: Hany_mss@mans.edu.eg (H. Mahanna), mahmoud.3zzab@gmail.com (M. Azab)*

Received 17 April 2019; Accepted 22 September 2019

ABSTRACT

This study aims mainly to use the soybean leaves (SL), agricultural wastes, as a new low-cost adsorbent for Reactive Red 195 (RR195) dye removal from aqueous solutions. The dried SL was chemically modified by acetic acid (AA) to improve its adsorption capacity. The adsorbent (AA-SL) was characterized by scanning electron microscopy (SEM) and Fourier transform infrared spectroscopy (FTIR). The effects of operational parameters such as contact time, pH, adsorbent dose, initial dye concentration, and temperature were investigated in batch experiments. Adsorption kinetics, isotherm, and thermodynamic of AA-SL have been studied. The AA-SL structure was found to be irregular and porous. FTIR revealed that the surface of AA-SL was abundant in various functional groups. The solution pH strongly affects RR195 removal efficiency. The highest removal efficiency equal to 97.8% was achieved using a solution pH equal to 1 at 50°C. The removal efficiency was increased by increasing the solution temperature. The adsorption of RR195 was decreased from 15.32 to 2.29 mg g^{-1} with increasing the adsorbent dose from 0.25 to 3 g L^{-1}, respectively. Increasing initial dye concentration from 5 to 40 mg L^{-1} resulted in increasing the adsorption capacity from 2.2 to 9.2 mg g^{-1}, respectively and decreasing the removal rate from 88% to 45.8%, respectively. The adsorption of RR195 onto AA-SL obeyed Langmuir (R^2 = 0.998) and D–R (R^2 = 0.967) models with a theoretical maximum adsorption capacity of about 12 mg g^{-1} at 50°C. The experimental data fitted very well with the pseudo-second-order kinetic (R^2 = 0.991). Thermodynamic studies indicated that the reaction is irreversible and endothermic adsorption. AA-SL, as a low-cost material has the potential to be used as a new alternative adsorbent for the removal of RR195 dye from aqueous solutions.

Keywords: Adsorption; Reactive red 195; Soybean leaves; Isotherm models; Kinetic study

1. Introduction

Industries such as textiles, paints, leather, pulp and paper, and plastics generate huge quantities of wastewater, due to the high consumption of water used in the dyeing processes [1,2]. The dye is one of the most dangerous chemical compounds found in effluent industrial wastewater [3,4]. More than 700,000 tons per year of dyes are produced all over the world [5]. Its persistence in water streams causes serious problems to the environment and living organisms such as affecting photosynthetic activity in aquatic life due to reduced light penetration. In addition, these compounds are toxic and have severe health risks to human beings [6–9]. The three main types of dyes are anionic (reactive, direct, and acid dyes), cationic (basic dyes), and non-ionic (dispersed dyes) [10]. Reactive dyes are one of the most prevalent types of dyes because they have high solubility in water and are easily hydrolyzed into an insoluble form. However, it is the most problematic among other dyes because it tends to pass through the treatment system unaffected [11,12].

The treatment of industrial effluents wastewater containing dyes is necessary before their final discharge to

* Corresponding author.

the environment. Several physical, chemical, and biological methods have been used for dye removal from wastewater effluents. Biological treatment methods such as fungal decolonization, microbial degradation, and microbial biomass adsorption are commonly used in decolorizing a wide range of dyes [13,14]. However, its application is limited because it requires a large land area and it is more sensitive toward any variations, and also toxic chemicals [15,16]. Chemical treatment methods include coagulation, flocculation, precipitation, electrochemical process, conventional oxidation by oxidizing agents and advanced oxidation [17–20]. The chemical methods are very costly, need chemical reagents and require disposal of accumulated sludge [21,22]. Physical treatment methods are widely used such as filtration, ion exchange and adsorption [23–26]. Among these methods, adsorption has vast attention due to its simplicity of design, high performance and suitable in operating without the production of hazardous end products [27–30]. Activated carbon is the most commonly applied adsorbent for dye removal because of its rational surface area and organized pore structure but it has a high cost. Therefore, developing of new inexpensive, locally available, and effective adsorbents are required [28,31]. Among different sorbents, clay and agricultural wastes have drawn a lot of attention from researches due to its low cost, availability, and content of different functional groups that increase the adsorption capacity [32,33].

This study aims to develop a new low-cost adsorbent from soybean leaves (SL), agricultural wastes, for the removal of Reactive Red 195 (RR195) dye from industrial wastewater. In addition, investigate the effect of operational parameters such as contact time, adsorbent dose, dye concentration, pH, and temperature onto the adsorption performance. Moreover, Isotherms, kinetic and thermodynamic models of adsorption are determined for the used adsorbent.

2. Materials and methods

2.1. Chemicals

RR195 dye is supplied by OH YOUNG INDUSTRIAL CO. LTD., (South Korea) and has been used without further purification. The chemical structure of the RR195 dye is shown in Fig. 1. NaOH and HCl (1 M) were used for pH adjustment. Acetic acid (AA) (purity 99.9%) was used for adsorbent modification. All of the chemicals used in the experiments were of analytical grade.

2.2. AA-SL preparation

Dried SL, agricultural wastes, were collected from a farm in Dakahlia Governorate, Egypt. The obtained leaves were cut into small pieces of 3 cm length and washed several times with distilled water to remove dust and impurities, and then dried in an oven at 105°C for 24 h. The dried leaves were ground and sieved with 100 mesh sieve.

The sieved soybean materials were chemically modified by AA. 20.0 g of SL was weighed, immersed in 200 ml of a solution containing 0.6 M of AA, and stirred at 500 rpm for 30 min at 20°C then the temperature was raised to 120°C for 90 min. After cooling, the obtained products were washed with distilled water to remove any excess AA. AA-SL were dried at 105°C until constant weight achieved and placed in a desiccator for further use.

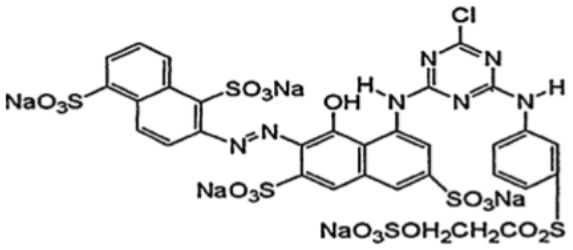

Fig. 1. Chemical structure of reactive red 195 dye.

2.3. AA-SL characterization

The Fourier transform infrared spectroscopy (FTIR) of the AA-SL was carried out using an FTIR spectroscopy (Thermo Scientific Nicolet IS10, USA) to identify the functional groups on the surface of AA-SL adsorbent. Infrared spectra were recorded in the range of 400–4,000 cm^{-1}. The surface structure of the AA-SL was observed using a scanning electron microscopy (SEM) (JEOL JSM-6510LV, Japan).

2.4. Solution preparation

RR195 dye was used to prepare a solution with different concentrations. By dissolving RR195 dye in distilled water, the dye-containing stock solution (500 mg L^{-1}) was developed. The desired concentrations of dye were prepared by diluting the stock solution. A spectrophotometer (Shimadzu UV-visible, 1601PC, Japan) was used to measure the dye concentration at a wavelength of 540 nm using a standard calibration curve.

2.5. Batch adsorption experiments

Batch adsorption experiments were conducted in 100 mL beakers to study the effect of operational parameters such as contact time (0–120 min), adsorbent dose (0.25–3 g L^{-1}), initial dye concentration (5–60 mg L^{-1}), pH (1–6), and temperature (25°C–50°C). The solution was stirred in a magnetic stirrer at 200 rpm until equilibrium was reached. The initial pH values of the solution were adjusted with HCl or NaOH using a pH meter. The solution after adsorption was centrifuged for 20 min at 3,000 rpm and supernatants were analyzed for remaining dye concentration using a spectrophotometer. The adsorption amount q_e (mg g^{-1}) and removal efficiency of RR195 at equilibrium was calculated as follows:

$$q_e\left(\frac{\text{mg}}{\text{g}}\right)=\frac{\left(C_0-C_t\right)V}{w} \tag{1}$$

$$\text{Dye Removal}\left(\%\right)=100\times\frac{\left(C_0-C_t\right)}{C_0} \tag{2}$$

where q_e (mg g^{-1}) is the dye adsorption capacity, C_0 and C_t (mg L^{-1}) are the initial dye concentration and dye

concentration at time t, respectively, V (L) is the solution volume, and w (g) is the adsorbent weight.

2.6. Adsorption isotherm

The adsorption isotherm is an important approach to evaluate the sorption capacity of adsorbents, also, to understanding how the adsorbent binds and interacts with the adsorbate [34]. In this work, several adsorption isotherm models have been studied to illustrate the equilibrium nature of adsorption. Langmuir, Freundlich, Temkin, and D–R isotherm equations were used to fit the experimental data and the constant parameters were calculated for each model.

Langmuir isotherm model has been applied, which assumes monolayer sorption onto a surface with a finite number of identical sites [22,35]. The Langmuir theory is represented as shown in Eq. (3).

$$\frac{C_e}{q_e} = \frac{1}{Q_m \times K_L} + \frac{C_e}{Q_m} \tag{3}$$

where C_e is the equilibrium concentration of dye in the solution (mg L^{-1}), q_e is the amount of dye adsorbed at equilibrium (mg g^{-1}), Q_m is the theoretical maximum amount of dye that can be adsorbed (mg g^{-1}), K_L is the Langmuir adsorption constant (L mg^{-1}).

Freundlich isotherm model assumes a heterogeneous adsorption surface that has unequal available sites with different energies of adsorption [25,35]. Freundlich adsorption isotherm can be expressed in the linear form as shown in Eq. (4).

$$\log q_e = \log K_F + \frac{1}{n}\log C_e \tag{4}$$

where K_F (L mg^{-1}) and n are isotherm constants indicate the capacity of the adsorbent and intensity of the adsorption, respectively.

Dubinin–Radushkevich (D–R) isotherm model is usually used to express the adsorption mechanism and to estimate adsorbent porosity characteristics and the apparent adsorption energy [24]. The linearized D–R isotherm model is expressed in Eq. (5).

$$\ln q_e = \ln Q_s - B\,\varepsilon^2 \tag{5}$$

where Q_s is the theoretical saturation capacity (mg g^{-1}), B is the D–R model constant ($mol^2\ J^{-2}$), ε is the Polanyi potential and is equal to

$$\varepsilon = RT\ln\left(1+\frac{1}{C_e}\right) \tag{6}$$

The mean energy of sorption, E (kJ mol^{-1}), is related to B as:

$$E = \frac{1}{\sqrt{2B}} \tag{7}$$

where R is the universal gas constant (8.314 J mol^{-1} K^{-1}), T is the solution temperature (K).

The Temkin isotherm model is based on the assumption that the adsorption heat would decrease linearly with the increase of adsorbent coverage [10]. The Temkin isotherm has usually been applied in linear form as in the following equations:

$$q_e = \frac{RT}{b_t}\ln K_t + \frac{RT}{b_t}\ln C_e \tag{8}$$

$$B = \frac{RT}{b_t} \tag{9}$$

where b_t is Temkin constant related to heat of sorption (J mol^{-1}), K_t is the Temkin isotherm equilibrium binding constant (L mg^{-1}).

2.7. Adsorption kinetics

To investigate the adsorption mechanism of RR195 onto AA-SL, kinetic models such as the pseudo-first-order model, pseudo-second-order model, and intraparticle diffusion model were used to fit the experimental data.

2.7.1. Pseudo-first-order model

The nonlinear form of the pseudo-first-order model is given by Eq.(10) and the integrated expression of this equation is expressed by Eq. (11).

$$\frac{dq_t}{dt} = k_1\left(q_e - q_t\right) \tag{10}$$

$$\log\left(q_e - q_t\right) = \log q_e - \frac{k_1}{2.303}t \tag{11}$$

where q_e and q_t are the amount of dye adsorbed on adsorbent at equilibrium and at time t, respectively (mg g^{-1}), and k_1 is the pseudo-first-order kinetic constant (min^{-1}).

2.7.2. Pseudo-second-order model

The linear form of the pseudo-second-order model is presented in Eq. (12).

$$\frac{t}{q_t} = \frac{1}{k_2 q_e^2} + \frac{1}{q_e}t \tag{12}$$

where k_2 (g mg^{-1} min^{-1}) is the pseudo-second-order rate constant.

2.7.3. Intraparticle diffusion model

The adsorption of RR195 onto AA-SL adsorbent may be controlled via either external film diffusion or the intraparticle diffusion or both [32]. To identify the diffusion mechanism, the Intraparticle diffusion model as presented in Eq. (13) is used.

$$q_t = k_d t^{0.5} + C \quad (13)$$

where q_t (mg g^{-1}) is the adsorption capacity at time t (min), k_d (mg g^{-1} min$^{-0.5}$)) is the intraparticle diffusion rate constant, and C (mg g^{-1}) is the intercept which represents the boundary layer thickness. A larger C value confirms a greater effect of the boundary layer [36].

2.8. Thermodynamic study

The enthalpy change ($\Delta H°$), entropy change ($\Delta S°$), and free energy change ($\Delta G°$) of RR195 adsorption onto AA-SL were calculated from the following equations:

$$\ln \frac{q_e}{C_e} = \frac{\Delta S°}{R} - \frac{\Delta H°}{RT} \quad (14)$$

$$\Delta G° = \Delta H° - T\Delta S° \quad (15)$$

where C_e is the equilibrium concentration of dye (mg L^{-1}), q_e is the amount of dye adsorbed at equilibrium (mg g^{-1}), R is the universal gas constant (8.314 J mol^{-1} K^{-1}), and T is the solution temperature (K).

3. Results and discussion

3.1. Adsorbent characterization

The surface morphology of AA-SL was demonstrated using the SEM. The SEM micrographs of AA-SL before and after the adsorption process are shown in Fig. 2. From Figs. 2a and b, the surface structures were irregular and it has several pores. These pores allowed a good surface for RR195 dye to be adsorbed. In Fig. 2c, it is obviously observed that the surface of AA-SL adsorbent was covered with dye ions, indicating that RR195 dye was successfully adsorbed onto the surface of AA-SL.

The FTIR spectra of AA-SL before and after dye adsorption are presented in Fig. 3. The high amount and various functional groups are identified on the surface of AA-SL adsorbent as shown in Fig. 3. The bands in the range of 520–672 cm^{-1} are associated with metal-oxygen and metal-hydroxyl vibrations [23]. The peak at 1,032 cm^{-1}is ascribed to C–O primary hydroxyl stretching [24]. Also, the bands at 1,241–1,459 cm^{-1} confirm the presence of C–O stretching and O–H bending [25]. The peaks from 1,518 to 1,543 cm^{-1} indicate the presence of C=C groups [4]. The bands in the range 1,650 to 1,919 cm^{-1} originated from C=O stretching [28]. While the characteristic peaks from 2,857 to 2,927 cm^{-1} are assigned to the hydrogen bond (C–H) [25]. Peaks ranging from 3,422 to 3,928 cm^{-1} can be attributed to the strong band vibration of O–H and N–H groups [6,28].

Those functional groups of AA-SL may significantly contribute to the adsorption of RR195 dye. After the adsorption process, It was obvious that the various peaks are shifted or disappeared, indicating that the functional groups on the AA-SL surface were covered or interacted with RR195 [10].

Therefore, the AA-SL characterization confirms that AA-SL has sufficient chemical and physical characteristics to adsorb RR195 dye.

3.2. Effect of contact time and temperature on RR195 removal

The contact time and temperature play a significant role in the dye adsorption process. The effect of contact time and

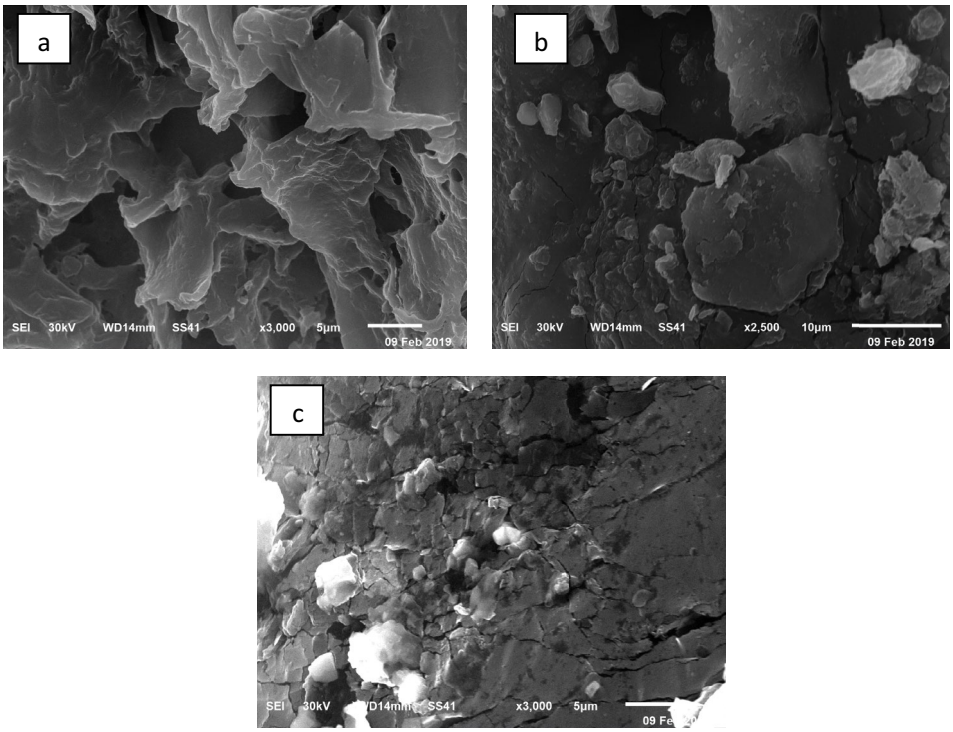

Fig. 2. SEM micrographs of AA-SL(a) before adsorption at 3,000×, (b) before adsorption at 2,500×, and (c) after adsorption at 3,000×.

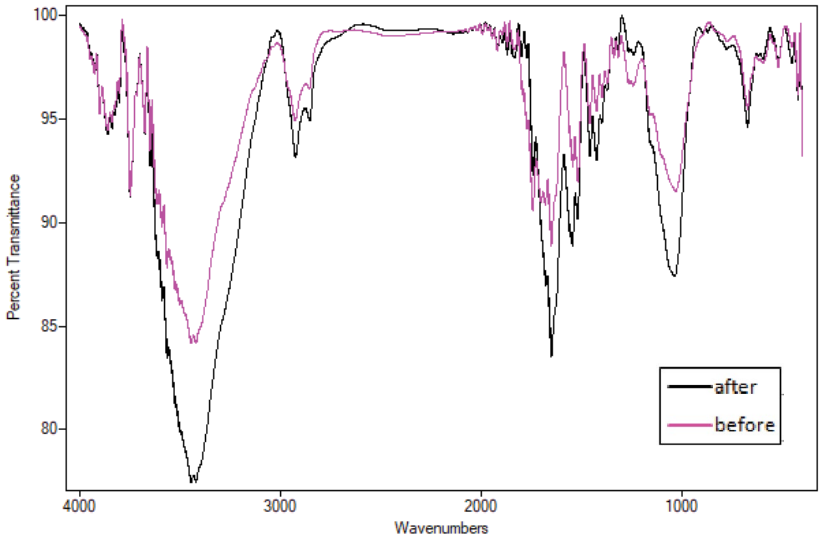

Fig. 3. FTIR spectra of AA-SL before and after the adsorption process.

temperature on the RR195 removal rate by AA-SL is illustrated in Fig. 4. RR195 removal rate is very fast during the first 30 min. From 30 to 90 min, a slight increase in removal rate occurs, and then reached equilibrium after 90 min of operation. The removal rate of RR195 was fast in the beginning because there are a large number of available AA-SL adsorption sites. The rate of adsorption decreases afterward, this may be due to the slow pore diffusion of the solute ion into the bulk of the AA-SL [21]. As shown in Fig. 4, a higher removal rate of RR195 was observed at higher temperatures. The removal rate was increased from 82.5% at 25°C to 97.8% at 50°C. The increase in removal rate of RR195 by increasing solution temperature is either due to an increase in binding sites onto AA-SL or to the higher affinity of sites for dye [2].

3.3. Effect of pH on RR195 removal

The pH is one of the most important parameters for adsorption studies especially for dye adsorption [37].

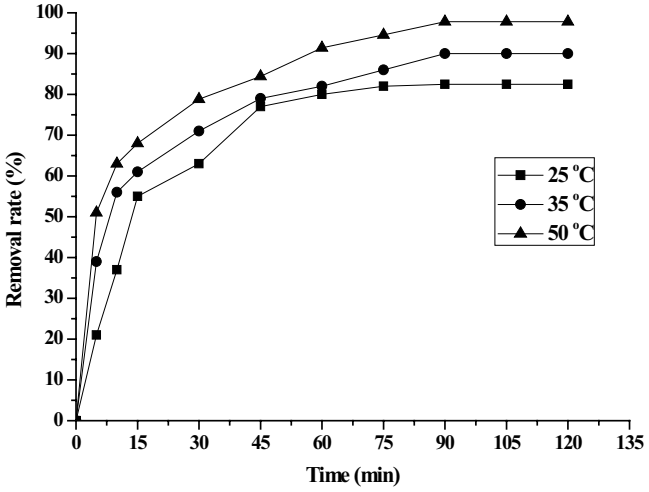

Fig. 4. Effect of contact time and temperature on RR195 removal rate (adsorbent dose = 2.0 g L^{-1}, pH = 1, and C_0 = 10 mg L^{-1}).

The effect of initial pH (range from 1 to 6) on the sorption of RR195 into AA-SL was carried out at a constant temperature of 25°C and initial dye concentration of 10 mg L^{-1} as shown in Fig. 5. The removal rate and adsorption capacity-achieved its highest values at pH equal to 1 (82.5% and 4.125 mg g^{-1}, respectively) and declined sharply with further increase in pH and reached to zero at pH equal to 4. A similar observation has been reported in the literature, shows that reactive dye biosorption decreases with increasing the pH [6]. This may be related to the electrostatic interactions between the negatively charged dye anion and the positively charged sorbent. With increasing pH, the number of positively charged sites decreases and the number of negatively charged sites increases [2].

3.4. Effect of AA-SL dose on RR195 removal

The effect of AA-SL dose on RR195 dye equilibrium adsorption and removal rate was investigated for a dye concentration of 10 mg L^{-1} and an adsorbent dose of 0.25–3 g L^{-1} at pH 2 and 25°C temperature as shown in Fig. 6. The removal rate of RR195 increased from 38.3% to 70% with increasing the adsorbent dose from 0.25 to 2 g L^{-1}, respectively. The main reason for this is that a larger dose of AA-SL increases the surface area of adsorbent and the number of active binding sites [35]. However, at high AA-SL dose more than 2 g L^{-1}, there is not any increase in the removal rate. This may be because the available number of dye molecules is insufficient in solution to bind with all existing active sites on the adsorbent which leads to surface saturation and an equilibrium condition as seen in Fig. 6 [11]. On the other hand, the adsorption capacity of RR195 was decreased from 15.32 to 2.29 mg g^{-1} with increasing the adsorbent dosage from 0.25 to 3 g L^{-1}, respectively. This could be ascribed to the fact that the adsorption sites remained unsaturated during the adsorption process [25] Another reason may be due to the particle interactive behavior, such as aggregation, resulted from high adsorbent dose. Such aggregation of AA-SL may lead to decrease in the total surface area

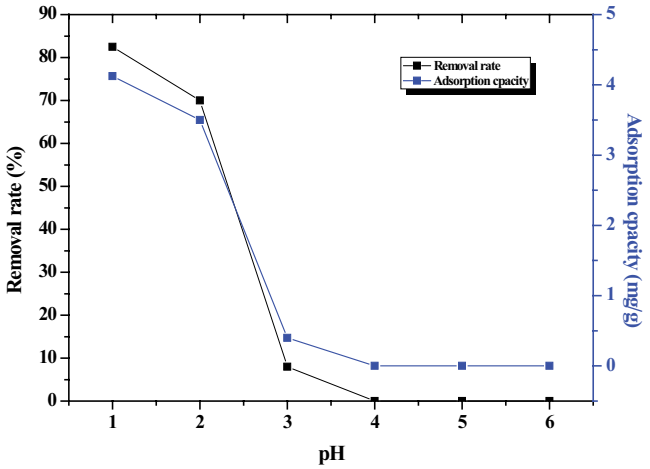

Fig. 5. Effect of pH on RR195 removal rate and adsorption capacity (C_0 = 10 mg L^{-1}, adsorbent dose = 2 g L^{-1}, contact time = 90 min, and temperature = 25°C).

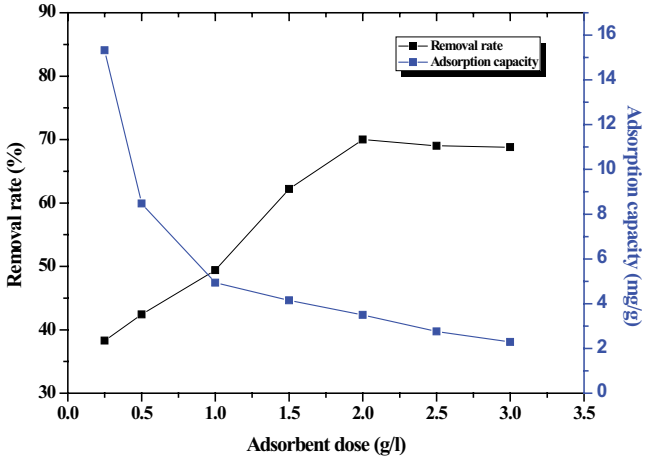

Fig. 6. Effect of AA-SL dose on RR195 removal rate and adsorption capacity (pH = 2, C_0 = 10 mg L^{-1}, contact time = 90 min, and temperature = 25°C).

available for adsorption and an increase in the diffusion path length [38].

3.5. Effect of Initial dye concentration on RR195 removal

The effect of initial concentration of RR195 (ranged from 5 to 60 mg L^{-1}) on the removal efficiency and adsorption capacity of AA-SL was investigated at pH 1 and 2 g L^{-1} adsorbent dose as shown in Fig. 7. It is obvious that high removal rate of RR195 was obtained at low initial dye concentrations where the removal rate was decreased gradually from 88% at 5 mg L^{-1} initial dye concentration to 45.8% at 40 mg L^{-1} initial dye concentration. This may be due to the shortage of available active sites required for the higher initial concentration of RR195. Similar results have been reported in literature [32,39]. However, increasing initial dye concentration from 5 to 40 mg L^{-1} resulted in increasing the adsorption capacity from 2.2 to 9.2 mg g^{-1}, respectively. This increase is due to the decrease in resistance to the uptake of solute from

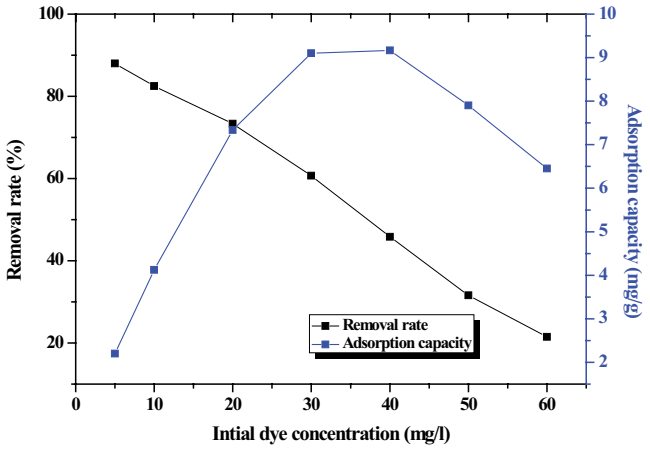

Fig. 7. Effect of Initial dye concentration on RR195 removal rate and adsorption capacity (pH = 1, adsorbent dose = 2 g L^{-1}, contact time = 90 min, and temperature = 25°C).

the RR195 solution. The initial concentration provides an essential driving force to overcome the mass transfer resistance of dye between the solid phases and aqueous [39,40].

3.6. Adsorption isotherm

The adsorption isotherm is characterized by certain constants that express the surface properties and the affinity of AA-SL towards RR195 dye. In the present study, four isotherm models are analyzed to investigate the suitable adsorption isotherm.

3.6.1. Langmuir isotherm

A plot of C_e vs. C_e/q_e for the removal of RR195 over AA-SL at different temperatures was developed to calculate the Langmuir isotherm constants which are shown in Fig. 8a. The Langmuir constant Q_m values were 8.54, 10.28, and 11.99 mg g^{-1} at 25°C, 35°C, and 50°C, respectively. The Langmuir constant K_L was found to be 1.186, 1.15, and 2.45 L mg^{-1} at 25°C, 35°C, and 50°C, respectively. The correlation coefficients (R^2) were in the range of 0.981 to 0.998 as shown in Table 1, which indicated that the adsorption process follows the Langmuir isotherm model. The value of Q_m increases with increasing temperature, which confirmed that the adsorption process is favored at higher temperatures.

3.6.2. Freundlich isotherm

The Freundlich adsorption isotherm constants were obtained from a linear plot of log C_e vs. log q_e at different temperatures as shown in Fig. 8b. Table 1 shows the Freundlich adsorption isotherm constants and correlation coefficients. The values of $1/n$ are 0.339, 0.336 and 0.266 at 25°C, 35°C, and 50°C, respectively. The values of $1/n$ were found to lie between zero and one for all investigated temperatures, which indicates that RR195 dye is favorably adsorbed by AA-SL adsorbent. By comparing the R^2 values for Langmuir and Freundlich models, The Langmuir model produced

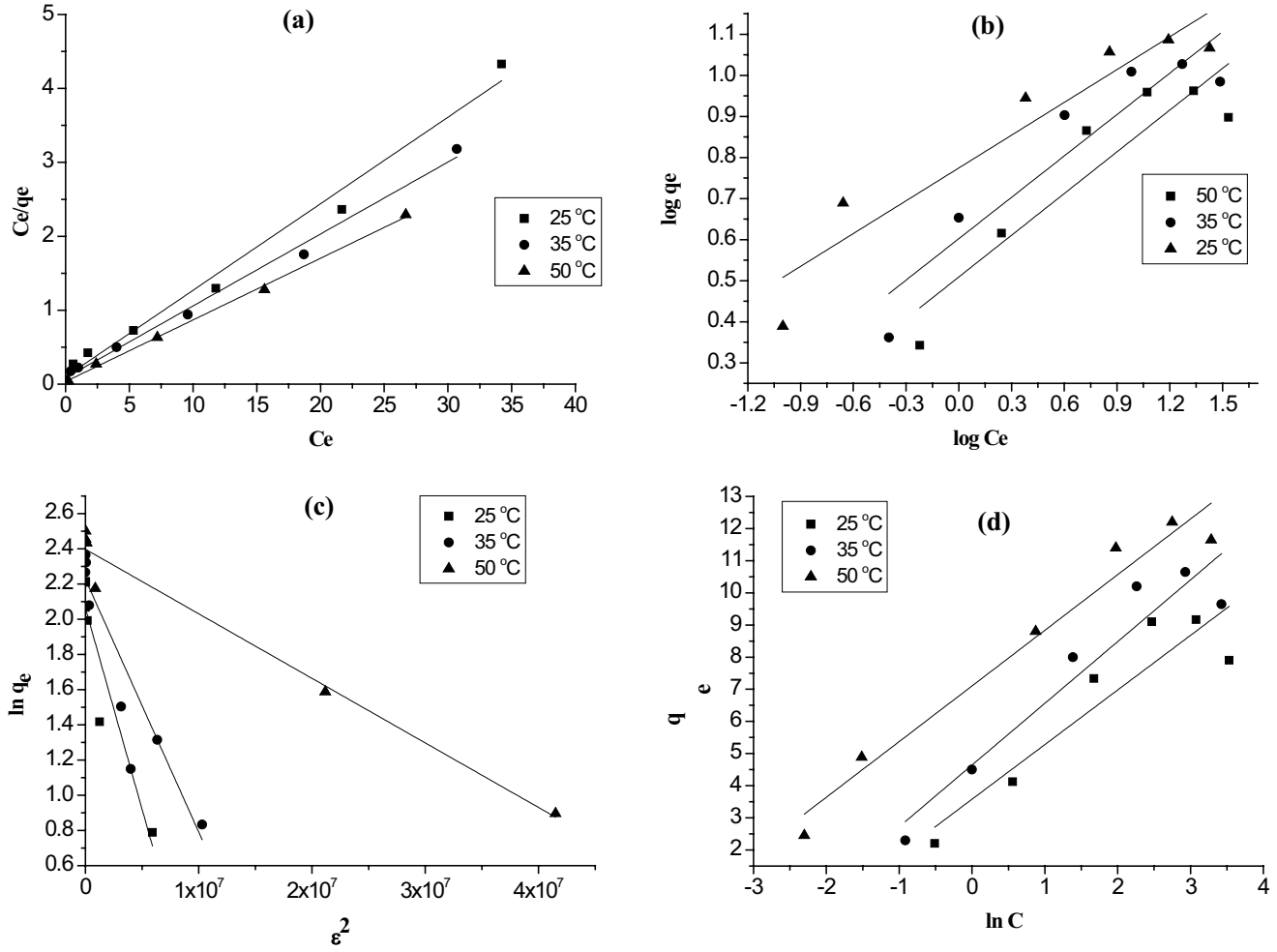

Fig. 8. Isotherm models for adsorption of RR195 dye by AA-SL at different temperatures (a) Langmuir, (b) Freundlich, (c) D–R, and (d) Temkin (pH = 1, adsorbent dose = 2 g L^{-1}, and contact time = 90 min).

a better fit for the experimental data than the Freundlich model.

3.6.3. D–R isotherm

Fig. 8c shows the linear plot between ε^2 vs. $\ln q_e$ at different temperatures. The calculated D–R constants and mean free energy for adsorption are shown in Table 1. The mean adsorption energy was in the range of 1.479 to 3.692 kJ mol^{-1}, which indicated that the adsorption process occurs physically. The D–R isotherm model fits well the experimental data depending on the correlation coefficient values as shown in Table 1.

3.6.4. Temkin isotherm

Temkin isotherm constants b_t and K_t were obtained from the plot of $\ln C_e$ vs. q_e at different temperatures as seen in Fig. 8d. The values of the Temkin constants and correlation coefficient are presented in Table 1. The obtained R^2 values for the Temkin model are 0.816, 0.894, and 0.957 at 25°C, 35°C, and 50°C, respectively, which indicated that the Temkin model fits the experimental data better than Freundlich model. However, the Temkin model is not as good as Langmuir and D–R isotherm models in fitting the data comparing the tabulated values of R^2 in Table 1.

The results of this work confirm that different isotherm models can be applied to describe the adsorption of RR195 onto AA-SL. However, Langmuir and D–R isotherm models are the best applicable forms.

3.7. Adsorption kinetics

3.7.1. Pseudo-first-order model

k_1 is determined from the slope of the plot of log $(q_e - q)$ vs. time. The first-order rate constants and the correlation coefficient values are presented in Table 2. It was observed that the pseudo-first-order model fits well the experimental data (R^2 = 0.972). Moreover, k_1 value is close to the values of previous researches [10,28,41]. This indicates that the pseudo-first-order model can be applied in a suitable way to describe the entire process of RR195 adsorption onto AA-SL adsorbent.

3.7.2. Pseudo-second-order model

From the slope and intercept of the plot of (t/q_t) vs. time, the parameters q_e and k_2 could be estimated. Based on Table 2, a Higher correlation coefficient (R^2) value of 0.991 was obtained for the pseudo-second-order model. In addition, the calculated equilibrium adsorption capacity (q_e) is consistent with the experimental data ($q_{e,exp.}$). This confirms the applicability of the pseudo-second-order model to interpret the experimental data.

Table 1
Constant parameters and correlation coefficients calculated for various adsorption isotherms models at different temperatures

Isotherm equation	Temperature		
	25°C	35°C	50°C
Langmuir			
Q_m (mg g^{-1})	8.54	10.28	11.99
K_L (L mg^{-1})	1.186	1.150	2.450
R^2	0.981	0.992	0.998
Freundlich			
$1/n$	0.339	0.336	0.266
K_F (L mg^{-1})	3.228	3.999	5.943
R^2	0.812	0.845	0.879
Dubinin–Radushkevich			
β (mol^2 J^{-2})	2.2854E-7	1.436E-7	3.668E-8
Q_s (mg g^{-1})	7.874	9.274	10.997
E (kJ mol^{-1})	1.479	1.866	3.692
R^2	0.858	0.917	0.967
Temkin			
K_t (L g^{-1})	8.22	11.21	60.58
b_t (mg g^{-1})	1458.73	1334.35	1552.99
B (J mol^{-1})	1.699	1.920	1.731
R^2	0.816	0.894	0.957

3.7.3. Intraparticle diffusion model

The constants and R^2 values are shown in Table 2 and these values confirm that the intraparticle diffusion process plays an important role in the adsorption of RR195 onto AA-SL adsorbent. But the obtained value of R^2 for the intraparticle diffusion model (0.900) was found to be less than that obtained for the other models.

Therefore, the obtained results from the kinetic models of the adsorption of RR195 onto AA-SL adsorbent indicated that the pseudo-second-order model can fit the experimental data better than other models.

3.8. Thermodynamic study

$\Delta S°$ and $\Delta H°$ could be obtained from the intercept and slope of Van't Hoff plot of $\ln(q_e/C_e)$ vs. $1/T$ (the plot is not shown) and $\Delta G°$ could be obtained from Eq. (15). The values of $\Delta H°$, $\Delta S°$, and $\Delta G°$ are presented in Table 3.

As shown in Table 3, $\Delta H°$, $\Delta S°$, and $\Delta G°$ were 72.9 kJ mol^{-1}, 250.7 J mol^{-1} K^{-1}, –1.845 kJ mol^{-1} at 298.15 K, respectively. The values of $\Delta G°$ were negative at all investigated temperatures, which indicates the spontaneous nature of adsorption of RR195 dye onto AA-SL [2,6]. The positive value of $\Delta H°$ confirms the endothermic nature of the adsorption process [42]. The positive value of $\Delta S°$ reflects that there is an increase in randomness at the solid/solution interface for the RR195 adsorption onto AA-SL [43].

4. Conclusion

Converting agricultural wastes such as dried SL to a new low-cost adsorbent (AA-SL) for the removal of RR195 dye was investigated. The AA-SL structure was found to be irregular and porous. FTIR analysis revealed the mechanism of RR195 adsorption and the number of functional groups on the surface of AA-SL. Contact time, temperature, pH, AA-SL dose, and initial dye concentration affect the adsorption process significantly. The removal rate of RR195 dye was increased from 82.5% to 97.8% by increasing temperature from 25°C to 50°C, respectively at optimum

Table 2
Kinetic parameters for the removal of RR195 onto AA-SL

Pseudo-first-order kinetic model			Pseudo-second-order kinetic model			Intraparticle diffusion model		
k_1	q	R^2	k_2	q	R^2	k_d	C	R^2
0.0645	4.62	0.972	0.0117	5.0916	0.991	0.4598	0.4775	0.900

Table 3
Thermodynamic parameters for the adsorption of RR195 on AA-SL

Temperature (K)	$\Delta H°$ (kJ mol^{-1})	$\Delta S°$ (J mol^{-1} K^{-1})	$\Delta G°$ (kJ mol^{-1})
298.15			–1.845
308.15	72.9	250.7	–4.352
323.15			–8.113

pH 1. The adsorption of RR195 was decreased from 15.32 to 2.29 mg g^{-1} with increasing the adsorbent dose from 0.25 to 3 g L^{-1}, respectively. Increasing initial dye concentration from 5 to 40 mg L^{-1} resulted in increasing the adsorption capacity from 2.2 to 9.2 mg g^{-1}, respectively and decreasing the removal rate from 88% to 45.8%, respectively. The equilibrium data agreed well with Langmuir (R^2 = 0.998) and D–R (R^2 = 0.967) isotherm equations. The pseudo-second-order model is the best description model (R^2 = 0.991) for adsorption kinetics. The adsorption process is spontaneous, endothermic, and irreversible according to thermodynamic study. It can be concluded that AA-SL has the potential to be used as a new alternative adsorbent for the removal of RR195 dye from aqueous solutions due to its availability and its low cost.

References

[1] X.-C. Jin, G.-Q. Liu, Z.-H. Xu, W.-Y. Tao, Decolorization of a dye industry effluent by *Aspergillus fumigatus* XC6, Appl. Microbiol. Biotechnol., 74 (2007) 239–243.

[2] O. Aksakal, H. Ucun, Equilibrium, kinetic and thermodynamic studies of the biosorption of textile dye (Reactive Red 195) onto *Pinus sylvestris* L., J. Hazard. Mater., 181 (2010) 666–672.

[3] M. Asgher, Biosorption of reactive dyes: a review, Water Air Soil Pollut., 223 (2012) 2417–2435.

[4] E.C. Lima, B. Royer, J.C.P. Vaghetti, N.M. Simon, B.M. da Cunha, F.A. Pavan, E.V. Benvenutti, R. Cataluña-Veses, C. Airoldi, Application of Brazilian pine-fruit shell as a biosorbent to removal of reactive red 194 textile dye from aqueous solution: kinetics and equilibrium study, J. Hazard. Mater., 155 (2008) 536–550.

[5] S. Ziane, F. Bessaha, K. Marouf-Khelifa, A. Khelifa, Single and binary adsorption of reactive black 5 and Congo red on modified dolomite: performance and mechanism, J. Mol. Liq., 249 (2018) 1245–1253.

[6] A.Y. Dursun, O. Tepe, Removal of Chemazol Reactive Red 195 from aqueous solution by dehydrated beet pulp carbon, J. Hazard. Mater., 194 (2011) 303–311.

[7] D.L. Zhao, W.M. Zhang, C.L. Chen, X.K. Wang, Adsorption of Methyl Orange dye onto multiwalled carbon nanotubes, Procedia Environ. Sci., 18 (2013) 890–895.

[8] J. Goscianska, M. Marciniak, R. Pietrzak, Mesoporous carbons modified with lanthanum(III) chloride for methyl orange adsorption, Chem. Eng. J., 247 (2014) 258–264.

[9] M. Iqbal, *Vicia faba* bioassay for environmental toxicity monitoring: a review, Chemosphere, 144 (2016) 785–802.

[10] M.E. Mahmoud, G.M. Nabil, N.M. El-Mallah, H.I. Bassiouny, S. Kumar, T.M. Abdel-Fattah, Kinetics, isotherm, and thermodynamic studies of the adsorption of reactive red 195 A dye from water by modified Switchgrass Biochar adsorbent, J. Ind. Eng. Chem., 37 (2016) 156–167.

[11] V. Belessi, G. Romanos, N. Boukos, D. Lambropoulou, C. Trapalis, Removal of Reactive Red 195 from aqueous solutions by adsorption on the surface of TiO_2 nanoparticles, J. Hazard. Mater., 170 (2009) 836–844.

[12] M. Kamranifar, M. Khodadadi, V. Samiei, B. Dehdashti, M. Noori Sepehr, L. Rafati, N. Nasseh, Comparison the removal of reactive red 195 dye using powder and ash of barberry stem as a low cost adsorbent from aqueous solutions: Isotherm and kinetic study, J. Mol. Liq., 255 (2018) 572–577.

[13] C.R. Holkar, A.J. Jadhav, D.V. Pinjari, N.M. Mahamuni, A.B. Pandit, A critical review on textile wastewater treatments: possible approaches, J. Environ. Manage., 182 (2016) 351–366.

[14] A. El Nemr, O. Abdelwahab, A. Khaled, A. El Sikaily, Biosorption of Direct Yellow 12 from aqueous solution using green alga *Ulva lactuca*, Chem. Ecol., 22 (2006) 253–266.

[15] O. Adedayo, S. Javadpour, C. Taylor, W.A. Anderson, M. Moo-Young, Decolourization and detoxification of methyl red by aerobic bacteria from a wastewater treatment plant, World J. Microbiol. Biotechnol., 20 (2004) 545–550.

[16] R.G. Saratale, G.D. Saratale, J.S. Chang, S.P. Govindwar, Bacterial decolorization and degradation of azo dyes: a review, J. Taiwan Inst. Chem. Eng., 42 (2011) 138–157.

[17] V. Khandegar, A.K. Saroha, Electrocoagulation for the treatment of textile industry effluent – a review, J. Environ. Manage., 128 (2013) 949–963.

[18] A. Bedolla-Guzman, I. Sirés, A. Thiam, J.M. Peralta-Hernández, S. Gutiérrez-Granados, E. Brillas, Application of anodic oxidation, electro-Fenton and UVA photoelectro-Fenton to decolorize and mineralize acidic solutions of Reactive Yellow 160 azo dye, Electrochim. Acta, 206 (2016) 307–316.

[19] L. Bilińska, M. Gmurek, S. Ledakowicz, Comparison between industrial and simulated textile wastewater treatment by AOPs – biodegradability, toxicity and cost assessment, Chem. Eng. J., 306 (2016) 550–559.

[20] A.K. Verma, R.R. Dash, P. Bhunia, A review on chemical coagulation/flocculation technologies for removal of colour from textile wastewaters, J. Environ. Manage., 93 (2012) 154–168.

[21] S. Gupta, B.V. Babu, Removal of toxic metal Cr(VI) from aqueous solutions using sawdust as adsorbent: equilibrium, kinetics and regeneration studies, Chem. Eng. J., 150 (2009) 352–365.

[22] M.T. Yagub, T.K. Sen, S. Afroze, H.M. Ang, Dye and its removal from aqueous solution by adsorption: a review, Adv. Colloid Interface Sci., 209 (2014) 172–184.

[23] H. Cherifi, B. Fatiha, H. Salah, Kinetic studies on the adsorption of methylene blue onto vegetal fiber activated carbons, Appl. Surf. Sci., 282 (2013) 52–59.

[24] Z. Noorimotlagh, R.D. Cheshmeh, A.R. Khataee, S. Shahriyar, H. Nourmoradi, Adsorption of a textile dye in aqueous phase using mesoporous activated carbon prepared from Iranian milk vetch, J. Taiwan Inst. Chem. Eng., 45 (2014) 1783–1791.

[25] Z. Qi, Q. Liu, Z. Zhu, Q. Kong, Q. Chen, S. Zhao, Y. Liu, M. Miao, C. Wang, Rhodamine B removal from aqueous solutions using loofah sponge and activated carbon prepared from loofah sponge, Desal. Wat. Treat., 57 (2016) 29421–29433.

[26] M. Riera-Torres, C. Gutiérrez-Bouzán, M. Crespi, Combination of coagulation-flocculation and nanofiltration techniques for dye removal and water reuse in textile effluents, Desalination, 252 (2010) 53–59.

[27] M. Rafatullah, O. Sulaiman, R. Hashim, A. Ahmad, Adsorption of methylene blue on low-cost adsorbents: a review, J. Hazard. Mater., 177 (2010) 70–80.

[28] N.S.A. Mubarak, A.H. Jawad, W.I. Nawawi, Equilibrium, kinetic and thermodynamic studies of Reactive Red 120 dye adsorption by chitosan beads from aqueous solution, Energy Ecol. Environ., 2 (2017) 85–93.

[29] N.E. Ibisi, C.A. Asoluka, Use of agro-waste (*Musa paradisiaca* peels) as a sustainable biosorbent for toxic metal ions removal from contaminated water, Chem. Int., 4 (2018) 52–59.

[30] V.K. Gupta, Suhas, Application of low-cost adsorbents for dye removal – a review, J. Environ. Manage., 90 (2009) 2313–2342.

[31] P. Sharma, H. Kaur, M. Sharma, V. Sahore, A review on applicability of naturally available adsorbents for the removal of hazardous dyes from aqueous waste, Environ. Monit. Assess., 183 (2011) 151–195.

[32] E.S.Z. El Ashtoukhy, *Loofa egyptiaca* as a novel adsorbent for removal of direct blue dye from aqueous solution, J. Environ. Manage., 90 (2009) 2755–2761.

[33] A. Kausar, M. Iqbal, A. Javed, K. Aftab, Zill-i-Huma Nazli, H.N. Bhatti, S. Nouren, Dyes adsorption using clay and modified clay: a review, J. Mol. Liq., 256 (2018) 395–407.

[34] U. Tezcan Un, F. Ates, Low-cost adsorbent prepared from poplar sawdust for removal of disperse orange 30 dye from aqueous solutions, Int. J. Environ. Sci. Technol., 16 (2019) 899–908.

[35] M.E. Mahmoud, G.M. Nabil, N.M. El-Mallah, S.B. Karar, Improved removal and decolorization of C.I. anionic reactive yellow 145 A dye from water in a wide pH range via active carbon adsorbent-loaded-cationic surfactant, Desal. Wat. Treat., 55 (2015) 227–240.

[36] F. Nekouei, S. Nekouei, I.J. Tayagi, V.K. Gupta, Kinetic, thermodynamic and isotherm studies for acid blue 129 removal

from liquids using copper oxide nanoparticle-modified activated carbon as a novel adsorbent, J. Mol. Liq., 201 (2014) 124–133.
[37] M.A.M. Salleh, D.K. Mahmoud, W.A.W.A. Karim, A. Idris, Cationic and anionic dye adsorption by agricultural solid wastes: a comprehensive review, Desalination, 280 (2011) 1–13.
[38] X.S. Wang, Y. Zhou, Y. Jiang, C. Sun, The removal of basic dyes from aqueous solutions using agricultural by-products, J. Hazard. Mater., 157 (2008) 374–385.
[39] O. Abdelwahab, Evaluation of the use of loofa activated carbons as potential adsorbents for aqueous solutions containing dye, Desalination, 222 (2008) 357–367.
[40] N.K. Amin, Removal of direct blue-106 dye from aqueous solution using new activated carbons developed from pomegranate peel: adsorption equilibrium and kinetics, J. Hazard. Mater., 165 (2009) 52–62.
[41] D. Chebli, A. Bouguettoucha, T. Mekhalef, S. Nacef, A. Amrane, Valorization of an agricultural waste, *Stipa tenassicima* fibers, by biosorption of an anionic azo dye, Congo red, Desal. Wat. Treat., 54 (2015) 245–254.
[42] Q. Kong, Y.N. Wang, L. Shu, M.S. Miao, Isotherm, kinetic, and thermodynamic equations for cefalexin removal from liquids using activated carbon synthesized from loofah sponge, Desal. Wat. Treat., 57 (2016) 7933–7942.
[43] Y.N. Wang, Q. Liu, L. Shu, M.S. Miao, Y.Z. Liu, Q. Kong, Removal of Cr(VI) from aqueous solution using Fe-modified activated carbon prepared from luffa sponge: kinetic, thermodynamic, and isotherm studies, Desal. Wat. Treat., 57 (2016) 29467–29478.